Generalization of the pair approximation and its application to $(Zn_{1-x}Mn_x)_3As_2$

H. Bednarski and J. Cisowski
Department of Solid State Physics, Polish Academy of Sciences, ulica Wandy 3, 41-800 Zabrze, Poland
(Received 17 February 1993)

By taking into account the results of recent studies of $(Zn_{1-x}Mn_x)_3As_2$ (ZMA), which is an example of a II-V diluted magnetic semiconductor (DMS) with a very complicated tetragonal crystal structure, we have generalized the pair-approximation model, widely used to analyze the magnetic behavior of II-VI DMS's, for an arbitrary structure. We have subsequently applied our model, which may be called the generalized pair approximation, to reinterpreting the results of magnetic measurements obtained for ZMA. Based on theoretical works that treat the Mn-Mn interaction in DMS's as a sum of superexchange and the Bloembergen-Rowland (BR) mechanism, we have been able to obtain satisfactory agreement between our approach and experiment by introducing only two adjustable parameters, in spite of the complexity of the crystal structure of ZMA. These parameters are the first nearest-neighbor exchange constants for both mechanisms and they have been found to be equal to -53 and -11 K for superexchange and the BR exchange, respectively.

I. INTRODUCTION

By alloying the II-V tetragonal semiconducting compound Zn_3As_2 with manganese, the $(Zn_{1-x}Mn_x)_3As_2$ (ZMA) system, belonging to the family of diluted magnetic (semimagnetic) semiconductors (DMS's or SMSC's), can be formed. Extensive studies of the magnetic properties of ZMA up to $x=0.14$ have been performed by Denissen *et al.*[1] An analysis of the experimental data obtained in this work has been done within the so-called extended nearest-neighbor pair approximation[2,3] (ENNPA), which is an extended version of the pair approximation as originally introduced by Matho[4] for canonical spin glasses: the difference between the approaches lies in the fact that the ENNPA takes into account not only the pairs of interacting paramagnetic ions, as does the pair approximation, but also the coupled triples. Apart from ZMA, the ENNPA has been first applied to $(Cd_{1-x}Mn_x)_3As_2$ (Ref. 2) (CMA) as well as to reinterpreting various experimental data obtained for Mn-alloyed II-V DMS's.[3] Subsequently, the pair approximation has been also used to analyze the magnetic properties of II-VI DMS's alloyed with Fe (Refs. 5 and 6) and, very recently, with Co.[7,8]

The analysis of the magnetic behavior of ZMA within the ENNPA (Ref. 1) was based on an idealized quasicubic (qc) crystal structure (see, e.g., Ref. 9) of the system, i.e., the Mn ions were assumed to be randomly located on an ideal simple-cubic (sc) cation sublattice, which implies only one NN Mn-Mn distance with a corresponding exchange constant J_1, a unique next-nearest-neighbor (NNN) distance with J_2, etc. In order to get a fair agreement between theory and experiment. Denissen *et al.*[1] have been forced to introduce four fitting parameters, i.e., three consecutive exchange constants ($J_1/k_B=-100$ K, $J_2/k_B=-20$ K, $J_3/k_B=-6$ K, with k_B the Boltzmann constant) and an additional parameter $J_0/k_B=-40$ K describing the long-range interaction of the type $J(r)=J_0r^{-n}$ (where r is a distance in units of the NN separation), with $n=4.5$ as found from an analysis of the spin-glass freezing temperature as a function of Mn concentration.

Quite recently, de Vries *et al.*[10,11] carried out a detailed structural study of the ZMA and found that the cation sublattice of this system is severely distorted, which results in 12 different values for the NN Mn-Mn distances instead of one, as assumed in Ref. 1; similarly, the number of NNN distances increases considerably (see Fig. 1).

Motivated by the above-mentioned works and also being involved in studies of Mn-allowed II-V DMS's,[12,13] we have undertaken an effort to generalize the pair approximation for an arbitrary crystal structure. The resulting model has been subsequently applied by us to reinterpreting the experimental data obtained so far for ZMA.[1,14,15] During the fitting procedure, we have made use of simple formulas describing the distance dependence of superexchange and Bloembergen-Rowland (BR) interactions, which are believed to be the most important exchange mechanisms in DMS's.[16,17]

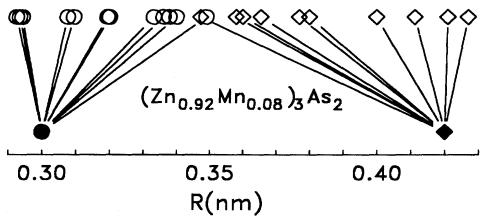

FIG. 1. Cation-cation distances in the real crystal structure of ZMA with $x=0.08$ (open symbols; Refs. 10 and 11) and in the quasicubic structure (solid symbols; Ref. 1). The transition from the former to the latter structure reduces 12 various distances (open circles) to one NN distance (solid circle) and 28 further distances (only a part of which is shown in the figure as open rhombs), also to one NNN distance (solid rhomb).

0163-1829/93/48(8)/5113(7)/$06.00

II. THEORY

The basic assumption of the pair approximation[4] is that the partition function of a macroscopic system with a fixed random distribution of spins (connected in the case of DMS's with the presence of paramagnetic ions in a host semiconducting lattice) may be factorized into contributions of pairs of spins. Thus, each spin is considered to belong to one pair formed with its nearest magnetic neighbor (NMN), which may be located on any lattice site, and spins belonging to different pairs are treated as noninteracting.

The Hamiltonian for a pair of spins in the presence of an external magnetic field **B** can be expressed in the Heisenberg form as

$$H_p = -g\mu_B(\mathbf{S}_i + \mathbf{S}_{\mathrm{NMN}_i})\cdot\mathbf{B} - 2J_i\mathbf{S}_i\cdot\mathbf{S}_{\mathrm{NMN}_i} , \tag{1}$$

where g is the Landé factor, μ_B is the Bohr magneton, and $J_i = J(R_i)$ is an exchange constant between spins $\mathbf{S}_i$ and $\mathbf{S}_{\mathrm{NMN}_i}$, separated by a distance R_i. Thus, the total interaction is given by

$$H = \sum_{\{i\}_p} H_p , \tag{2}$$

with the summation running over all pairs $\{i, \mathrm{NMN}_i\}$.

The magnetic properties of the system can be derived from the total free energy F, which, for the Hamiltonian expressed by Eqs. (1) and (2), reads

$$F = -\frac{k_B T}{2} \sum_{i=1}^{N} \ln \mathrm{Tr} \exp(-\beta H_p) , \tag{3}$$

where $\beta = (k_B T)^{-1}$, Tr denotes the trace over all spin degrees of freedom, and N is the total number of spins.

The above formula may be applied, in principle, to DMS's with paramagnetic ions of moderate concentration ($x \leq 0.1$) randomly distributed over a cation sublattice in which each cation site has the same arrangement of other cations, which results in a unique NN distance between the ions; this includes most of the known II-VI DMS's crystallizing in the zinc-blende structure. For a more complicated structure, there may be a few inequivalent cation sites yielding a number of NN distances. For example, in the wurtzite structure there are two different NN distances (clearly evidenced in recent magnetization experiments performed on $Cd_{1-x}Mn_xS$ (Ref. 18), while in the case of ZMA there are 12 such distances.[11] Assuming now that, for an arbitrary crystal structure, the paramagnetic ions with spin **S** may occupy t kinds of inequivalent sites and treating the sites of the host lattice as being arranged in spheres around the reference site, we can generalize Eq. (3) to obtain

$$F = \frac{N}{2t} \sum_{j=1}^{t} \sum_{\nu_j}^{\infty} P_{\nu_j}(x) F_{\nu_j} , \tag{4}$$

with $\sum_{\nu_j} P_{\nu_j}(x) = 1$, where

$$F_{\nu_j} = -k_B T \ln \mathrm{Tr} \exp\{\beta[g\mu_B(\mathbf{S}_{\nu_j} + \mathbf{S})\cdot\mathbf{B} + 2J_{\nu_j}\mathbf{S}_{\nu_j}\cdot\mathbf{S}]\} \tag{5}$$

is the free energy of a pair of interacting spins, and $P_{\nu_j} = N_{\nu_j}/N_j$ is the probability of finding such a pair, given by

$$P_{\nu_j}(x) = (1-x)^{m_{\nu_j - 1}} - (1-x)^{m_{\nu_j}} , \tag{6}$$

where $m_{\nu_j} = \sum_{\tau_j} M_{\tau_j}$ with M_{τ_j} being the number of sites in τ_jth sphere.

For structures with only one kind of cation sites, i.e., for $t = 1$, Eqs. (4)–(6) reduce to those found previously;[1–4] therefore, our approach may be called the generalized pair approximation (GPA).

Based on Eqs. (4)–(6), one can derive the other thermodynamic quantities, such as the magnetic specific heat ($C_m = -T[\partial^2 F/\partial T^2]_B$), magnetization ($M = -[\partial F/\partial B]_T$), and susceptibility ($\chi = -[\partial^2 F/\partial B^2]_T$), and compare them with experimental data, as will be shown in Sec. IV.

III. CRYSTAL STRUCTURE OF $(Zn_{1-x}Mn_x)_3As_2$

As follows from the works of de Vries *et al.*,[10,11] the crystal structure of ZMA, at least for $0 \leq x \leq 0.135$ and at $T \leq 300$ K, is isomorphic with the α phase of Zn_3As_2 (space group $I4_1cd$). The tetragonal unit cell of α-Zn_3As_2, containing 160 atoms (96 Zn and 64 As), can be divided into 16 fluorite cubes provided that $c_t \cong 2a_t$, where $a_t = 11.78$ Å and $c_t = 23.64$ Å are the tetragonal lattice constants. Each fluorite cube contains four As atoms on an fcc lattice (the lattice constant $a \cong a_t/2$) and six Zn atoms inside the cube on a distorted sc lattice (the lattice constant $\approx a/2$), with two vacancies connected by a body diagonal. Thus, in the real structure of α-Zn_3As_2, there are six types of inequivalent cation sites which, in the case of ZMA, may be occupied at random by Mn ions, and volume per one cation site is equal to $a^3/6$.

Such a complex crystal structure has been oversimplified by Denissen *et al.*[1] in two steps. First, the distortion of the cation sublattice has been neglected, which reduces the number of inequivalent cation sites from 6 to 3 and gives the unique NN distance equal to $a/2$. Second, due to the particular arrangement of vacancies in the lattice, each of those three inequivalent cation sites may have 3, 4, or 5 NN's and 9, 9, or 10 NNN's; this has been arithmetically averaged to get only one kind of cation site, i.e., the quasicubic structure, with 4 NN's and 9.33 NNN's.[19]

Comparison between cation-cation distances in the qc structure and in the real structure of ZMA is shown in Fig. 1. It can be seen that, for the real structure, there is a quasicontinuous spectrum of possible Mn-Mn distances with even some overlap of NN and NNN spheres,[11] while for the qc structure, those spheres are very well separated. It is also worthwhile to mention that the first NN separation ($R_1 \approx 3$ Å) is, to our knowledge, the smallest one among the known DMS's.

IV. APPLICATION OF THE GENERALIZED PAIR APPROXIMATION TO $(Zn_{1-x}Mn_x)_3As_2$

As follows from Eq. (4), the total free energy F within the GPA is a sum of free energies of pairs of interacting

spins multiplied by appropriate probabilities, which can be easily calculated for a given x provided the crystal structure of the system in question is known. Thus, in order to calculate F, one needs to specify an exchange constant for every type of pair. From the very beginning of our work, we have realized that we cannot follow the fitting procedure of Ref. 1 simply by increasing the number of the exchange constants as adjustable parameters (12 for NN's, 28 for NNN's, etc.), since then the procedure itself would become meaningless; instead, we must search for a distance dependence of the interaction strengths. Therefore, we have made use of theoretical studies of DMS's by Larson *et al.*[16] who have stated that antiferromagnetic superexchange, i.e., an indirect Mn-Mn exchange mediated by the anion, plays the dominant role with a minor contribution of the other indirect process, the Bloembergen-Rowland exchange, induced by the virtual interband transitions. As follows from Ref. 16, the superexchange constant $J^{\mathrm{SE}}(R)$ can be written as

$$J^{\mathrm{SE}}(R)=-U_{\mathrm{el}}f(R/a)\ , \tag{7}$$

where U_{el} depends on the electronic-structure details of a particular material and $F(R/a)$ (with a the lattice constant) is the material-insensitive function approximated by

$$f(R/a)=51.2\exp(-5.16R^2/a^2)\ . \tag{8}$$

In the case of the BR mechanism, the corresponding exchange constant $J^{\mathrm{BR}}(R)$ has the form[20,21]

$$J^{\mathrm{BR}}(R)=I^{\mathrm{BR}}R^{-3}\exp(-\alpha'_{\mathrm{BR}}R)\ , \tag{9}$$

where I^{BR} is a constant and $\alpha'_{\mathrm{BR}}=(2m_eE_g)^{1/2}/\hbar$, with m_e and E_g the electron effective mass and the energy gap, respectively.

Rearranging Eqs. (7)–(9) in order to express them as a function of $r=R/R_1$, i.e., in units of the first NN distance R_1 and the first NN exchange constants J_1^{SE} and J_1^{BR}, we get

$$J^{\mathrm{SE}}(r)=J_1^{\mathrm{SE}}\exp[-\alpha_{\mathrm{SE}}(r^2-1)]\ , \tag{10}$$

$$J^{\mathrm{BR}}(r)=J_1^{\mathrm{BR}}r^{-3}\exp[-\alpha_{\mathrm{BR}}(r-1)]\ , \tag{11}$$

where $\alpha_{\mathrm{SE}}=5.16R_1^2/a^2$ and $\alpha_{\mathrm{BR}}=R_1(2m_eE_g)^{1/2}/\hbar$, with, in the case of ZMA, $m_e=0.04m_0$ (m_0 is the free-electron mass) and $E_g=1.1$ eV.[1,22]

Thus, the total interaction strength $J(R)$ is given by

$$J(R)=J^{\mathrm{SE}}(R)+J^{\mathrm{BR}}(R) \tag{12}$$

and contains only two unknown parameters (J_1^{SE} and J_1^{BR}) which are to be found from a fit of the theoretical dependences obtained with the GPA to the experimental data.

The other parameters needed in calculations are the Landé factor g taken, as for other Mn-alloyed DMS's, as $g=2$, and the spin S of Mn ions. As for the latter, we have put its average value $S_{\mathrm{av}}=2.25$ in order to account for the magnetization and susceptibility data which show that, in the limit of vanishingly small Mn content, the saturation magnetization of ZMA is smaller than $5\mu_B$, as expected for the Mn^{2+} ion with $S=2.5$ in the ground state; this diminution is attributed to the p-d hybridization.[1,16,23]

When calculating the total free energy, the summation over the spheres [see Eq. (4)] has been carried out in such a way that $\sum_{\nu_j}P_{\nu_j}(x)\geq 0.995$; this condition requires taking into account up to 200 spheres.

The best overall fit of the GPA to the experimental data, as presented in Figs. 2–5, has been obtained for $J_1^{\mathrm{SE}}/k_B=-53$ K and $J_1^{\mathrm{BR}}/k_B=-11$ K, which give the total first NN exchange constant $J_1/k_B=-64$ K. We will return to this point at the end of this section, discussing first the comparison between theory and experiment for particular thermodynamic functions in greater detail. For the purpose of comparison we have inserted in Figs. 2 and 5 the results of calculations within the ENNPA as performed in Ref. 1 with four exchange constants as fitting parameters (in the case of Figs. 3 and 4 both the GPA and the ENNPA give practically the same curves). At first glance, both approaches seem to give comparably good descriptions of the experimental data, but our model is better in the sense that, on the one hand, we have taken into account the real crystal structure of ZMA and, on the other hand, we have used only two exchange constants as adjustable parameters.

A. Magnetic specific heat

The magnetic-specific-heat data[1] along with the theoretical curves are shown in Figs. 2 and 3. It can be seen that the GPA describes quite well the experimental data: Some deviation is observed at low temperatures and is most probably due to the strong assumption of the pair approximation restricting the Mn-Mn interaction within the pairs; thus, larger clusters of Mn ions and interactions between the pairs are neglected. In principle, in order to get better agreement, one could follow Refs.

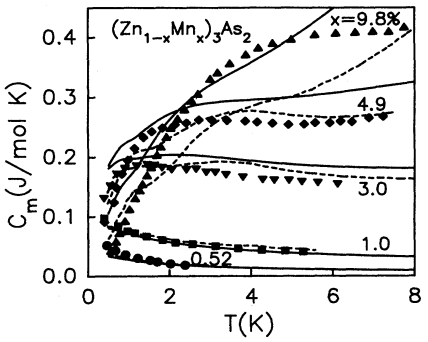

FIG. 2. The magnetic specific heat of ZMA in zero field. Experimental data and the dashed lines calculated within the extended nearest-neighbor pair approximation for $J_1/k_B=-100$ K, $J_2/k_B=-20$ K, $J_3/k_B=-6$ K, and $J(r)/k_B=-40r^{-4.5}$ K are taken from Ref. 1. The solid lines represent our calculations within the generalized pair approximation and taking into account superexchange and the Bloembergen-Rowland mechanism described by Eqs. (10)–(12) with $J_1^{\mathrm{SE}}/k_B=-53$ K and $J_1^{\mathrm{Br}}/k_B=-11$ K.

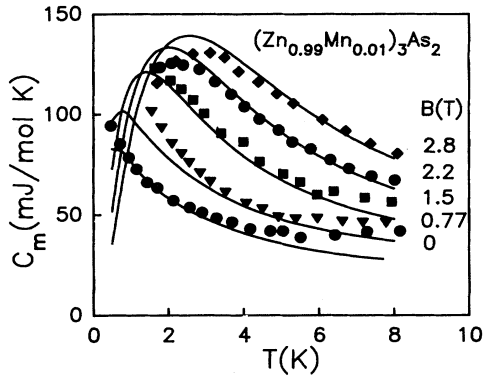

FIG. 3. The magnetic specific heat of ZMA with $x=0.01$ at various fields. The data of Ref. 1 and the solid lines are calculated in the same way as in Fig. 2.

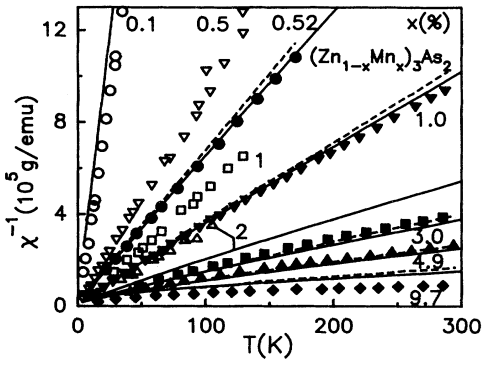

FIG. 5. The inverse susceptibility of ZMA: The data of Ref. 1, solid symbols, Ref. 14, open symbols. The dashed and solid lines have the same meaning as in Fig. 2.

1–3 by taking into account the coupled triples, but such a task would be very difficult, keeping in mind the complex crystal structure of ZMA, which leads to a very great number of different kinds of triples.

B. Magnetization

The high-field magnetization data[1] and corresponding GPA lines are shown in Fig. 4. As can be seen, irrespective of the Mn content, magnetization changes smoothly with magnetic field and does not exhibit any steplike structure in the field range investigated. As is known, the steps occur, for a given exchange constant J_n, at fields $B_{n,l}$ determined by the condition $g\mu_B B_{n,l}=2l|J_n|k_B$, with $l=1-5$, and should be observable if $k_BT\ll 2|J_n|$; the width of the steps is proportional to temperature, while their magnitude is proportional to the probability of finding a pair of spins coupled by the exchange interaction with a constant J_n.[24,25]

The absence of any steplike increase of magnetization in ZMA at fields up to 30 T has led Denissen *et al.*[1] to the conclusion that

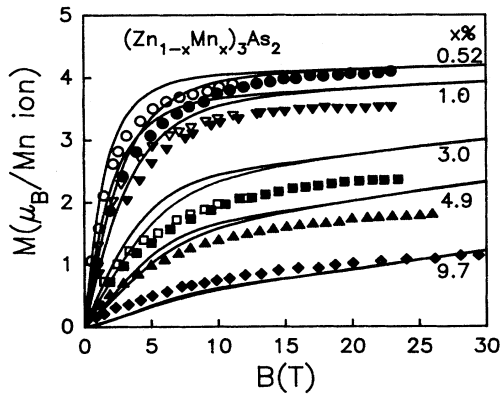

FIG. 4. The high-field magnetization of ZMA collected at $T=2$ K (open symbols) and at $T=4.2$ K (solid symbols). The data of Ref. 1 and the solid lines are calculated in the same way as in Figs. 2 and 3.

$$|J_1/k_B|>|J_2/k_B|>20\ \text{K}\ .$$

However, the lack of steps is not surprising, if we take into account, on the one hand, the great number of NN (12) and NNN (28) pairs occurring in the real structure (see Fig. 1) with the equal number of corresponding exchange constants and, on the other hand, a very small probability of finding a particular kind of the pair of spins which, on the whole, may give no observable steps in the field and temperature ranges investigated, even if the absolute values of exchange constants are much lower than those mentioned above.

C. Susceptibility

The temperature dependence of the inverse susceptibility, measured at $B=1.2$ T and corrected for the diamagnetic contribution of Zn_3As_2[1], along with the theoretical lines are shown in Fig. 5. Apart from the data of Ref. 1, we have also inserted in this figure the very recent results obtained for ZMA with $0.001\le x\le 0.02$ and measured at $B=0.01-0.02$ T;[14] the observed difference between the two sets of results for the same or similar Mn content may be due to the uncertainty in the crystal composition[25] and/or the presence of another paramagnetic element introduced unintentionally during the crystal growth.[26,27]

At higher temperatures, the data follow straight lines in accordance with the high-temperature series expansion of susceptibility leading to the Curie-Weiss law of the form[23]

$$\chi^{-1}=T/C-\theta/C\ , \tag{13}$$

with the Curie constant

$$C=xN_Ag^2\mu_B^2S(S+1)/k_BM\ ,$$

where N_A is Avogadro's number and M is the molecular weight, and with the Curie-Weiss temperature

$$\theta=2xS(S+1)\sum_p z_pJ_p/3k_B\ ,$$

where z_p is the number of cation sites on consecutive

coordination spheres. An interesting feature of Eq. (13) is that the ratio θ/C, which can be determined from experiment, contains all interactions but does not depend on x and S. Therefore, we have performed our fitting procedure in such a way that we get the experimental result ($\sum_p z_p J_p/k_B = -480$ K), while the procedure of Ref. 1 gives for this sum -630 K.

D. Spin freezing

The low-field susceptibility measurements of DMS's at sufficiently low temperatures reveal the presence of a cusp or kink, interpreted as a transition from the paramagnetic to the spin-glass state (see, e.g., the review papers, Refs. 28 and 29) and the corresponding temperature T_f, known as the freezing temperature, which strongly depends on the concentration of paramagnetic ions x, as shown in Fig. 6 for the case of ZMA.[1] It appears that the experimental data behave approximately as $T_f(x) \sim x^{n/3}$, with $n = 4.5$; such a dependence can be explained by assuming a long-range exchange interaction of the type $J(R) \sim R^{-n}$ and using the scaling argument which combines the average distance between paramagnetic ions $R_{\rm av}$ with their concentration x by the equation $R_{\rm av}^3 x = \text{const}$ together with the conjecture that T_f is related to the interaction energy at $R_{\rm av}$ by[29]

$$k_B T_f \approx J(R_{\rm av}) S(S+1) . \tag{14}$$

Within our model, we can try to describe the experimental $T_f(x)$ relationship by making use of the radial dependence of the exchange interaction as found from the analysis of the thermodynamic properties performed above. An example of such dependence for ZMA with $x = 0.08$, clearly demonstrating the role of both superexchange and the BR mechanism, is shown in Fig. 7. It can be observed that superexchange is dominant to about 5.5 Å and quickly vanishes with increasing distance; as for the BR mechanism, its contribution to the total exchange is not negligible even at short distances and becomes dominant at larger distances in spite of the fact that the energy gap of ZMA is relatively wide ($E_g = 1.1$ eV).

Having determined the $J(R)$ dependence, we will analyze the spin-glass transition in ZMA combining the approaches of Refs. 30 and 8. As is known,[30] the spin-glass freezing condition is based on the existence of a critical fraction of ions blocked or frozen by coupling with their magnetic neighbors if the exchange energy between two neighboring ions with spins $\mathbf{S}_1$ and $\mathbf{S}_2$ is larger than the thermal energy $k_B T$. On the other hand, there may exist a certain number of free ions, and such an ion is considered to be free if it has no magnetic neighbor inside the sphere of a radius R_f determined by

$$k_B T_f = 2J(R_f) \langle \mathbf{S}_1 \mathbf{S}_2 \rangle , \tag{15}$$

where $\langle \mathbf{S}_1 \mathbf{S}_2 \rangle$ is the pair-correlation function [equal to $-S(S+1)$, as in Eq. (14) in the fully aligned limit][8] which follows from the pair Hamiltonian [see Eq. (1) for $B = 0$] and reads

$$\langle \mathbf{S}_1 \mathbf{S}_2 \rangle = \frac{\mathrm{Tr}[\mathbf{S}_1 \mathbf{S}_2 \exp(2\beta J \mathbf{S}_1 \mathbf{S}_2)]}{\mathrm{Tr} \exp(2\beta J \mathbf{S}_1 \mathbf{S}_2)} . \tag{16}$$

The probability that a particular ion is free is given by

$$P_{\rm free} = (1-x)^{m_f} , \tag{17}$$

where $m_f = 4\pi R_f^3/3A$ is the total number of cation sites inside a sphere of the volume of $4\pi R_f^3/3$ and A is volume per one cation site, which is equal, in the case of ZMA, to $a^3/6$ (where $a \approx 6$ Å; see Sec. III).

The above equations together with the $J(R)$ dependence as given by Eqs. (10)–(12) have allowed us to calculate numerically the $T_f(x)$ relationship for certain values of $P_{\rm free}$. As pointed out by Twardowski *et al.*,[30] the choice of $P_{\rm free}$ is not a crucial point of their approach, especially for low probabilities; therefore, we have adopted the value of $P_{\rm free} = 2 \times 10^4$, as estimated by Escorne and Mauger,[31] and the result of our calculations is shown in Fig. 6 as the solid line.

It can be seen that, in spite of an exponential character

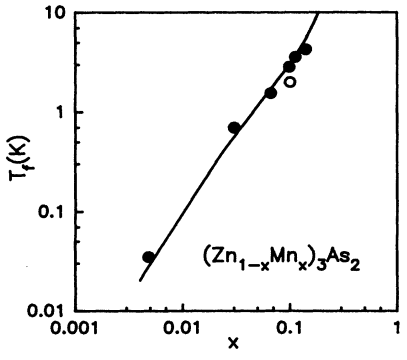

FIG. 6. The spin-freezing temperature of ZMA as a function of Mn concentration: The data of Ref. 1, solid circles, Ref. 15, open circle. The solid line is calculated according to Eqs. (15)–(17).

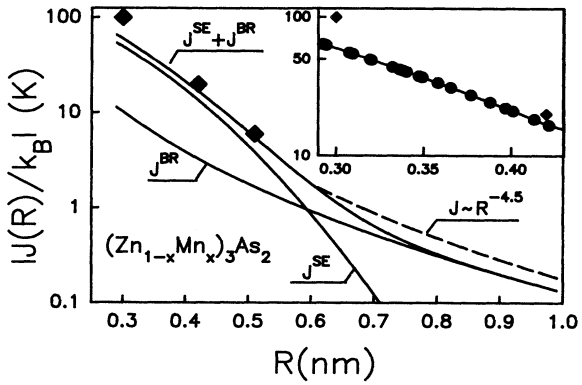

FIG. 7. The distance dependence of superexchange, the BR exchange, and their sum in ZMA with $x = 0.08$ deduced from our approach (solid curves) with the real crystal structure taken into account, as indicated by circles in the inset (showing the total interaction strengths at short distances in greater detail). The solid rhombs and the dashed line are the result of a fitting procedure of Ref. 1 for the quasicubic structure.

of the formulas describing both superexchange and the BR mechanism, the resulting curves, which reproduce the experimental data very well, are quite close to straight lines, obtained when adopting a phenomenological power-law dependence of the type $J(R) \sim R^{-n}$, which, however, has no theoretical background.

V. SUMMARY AND FINAL REMARKS

We have generalized the pair approximation, which is applicable, in principle, to simple crystal structures (in which each cation site has the same arrangement of other cations), for an arbitrary structure. The resulting model, which may be called the generalized pair approximation, has been subsequently applied by us to reinterpreting the results of magnetic measurements obtained so far for $(Zn_{1-x}Mn_x)_3As_2$ (Refs. 14 and 15), a tetragonal DMS with a complicated crystal structure, characterized by a quasicontinuous spectrum of possible Mn-Mn distances,[10,11] and a great number of NN's (12), NNN's (28), etc. This fact excludes treating the corresponding exchange constants as adjustable parameters and therefore we have made use of the recent theoretical works indicating that there are two essential Mn-Mn exchange mechanisms in DMS's, i.e., superexchange and the Bloembergen-Rowland exchange.[16,17] Applying simple formulas to describe the distance dependence of both mechanisms[16,20,21] and treating them as being additive, we have obtained satisfactory agreement between our approach and experimental data of the specific heat, magnetization, and susceptibility by introducing only two fitting parameters, the first NN exchange constant for superexchange ($J_1^{SE}/k_B = -53$ K) and the BR exchange ($J_1^{BR}/k_B = -11$ K). This gives the total first NN constant $J_1/k_B = -64$ K, which differs substantially from that found previously ($J_1/k_B = -100$ K) (Ref. 1) but is still higher than the values of the exchange constant ($J_1/k_B \approx -10$ K) found for Mn-alloyed II-VI compounds.[25,29] This fact, however, is not surprising, if one takes into account the difference between the NN separation of both systems: for ZMA, we have $R_1 \approx 3$ Å, while, for example, for $Cd_{1-x}Mn_xTe$ (CMT), $R_1 \approx 4.6$ Å. For the latter distance, our calculation gives $J_1 = -11$ K (see Fig. 7), which becomes comparable with $J_1 \approx -7$ K, as found for CMT,[25,29] and the remaining difference may be ascribed to a higher degree of p-d hybridization in II-V than in II-VI DMS's alloyed with manganese.[1]

The $J(R)$ dependence obtained by us also appears to be very useful in analysis of the $T_f(x)$ relationship, indicating a non-negligible role of the BR-type exchange even in wide-gap materials such as ZMA. On the other hand, we realize that the analytical formulas used by us to describe the radial dependence of superexchange and the BR mechanism may not be completely correct and require further improvements, as discussed for many years in theoretical works devoted to this difficult problem.[16,17,32–36] Nevertheless, based on very good agreement between our approach and experiment, we believe that these simple formulas reflect the main features of the interaction strengths in DMS's, confirming the commonly accepted theoretical prediction that superexchange is the main exchange mechanism at short distances but that it may be also stated that the role of the usually neglected BR-type mechanism of interaction is also of importance, especially at larger distances.

[1] C. J. M. Denissen, S. Dakun, K. Kopinga, W. J. M. Jonge, H. Nishihara, T. Sakakibara, and T. Goto, Phys. Rev. B **36**, 5316 (1987).

[2] C. J. M. Denissen, H. Nishihara, J. C. van Gool, and W. J. M. de Jonge, Phys. Rev. B **33**, 7637 (1986).

[3] C. J. M. Denissen and W. J. M. de Jonge, Solid State Commun. **59**, 503 (1986).

[4] K. Matho, J. Low Temp. Phys. **35**, 165 (1979).

[5] A. Twardowski, H. J. M. Swagten, T. F. H. van de Wetering, and W. J. M. de Jonge, Solid State Commun. **65**, 235 (1988).

[6] H. J. M. Swagten, A. Twardowski, W. J. M. de Jonge, and M. Demianiuk, Phys. Rev. B **39**, 2568 (1989).

[7] A. Lewicki, A. I. Schindler, I. Miotkowski, B. C. Crooker, and J. K. Furdyna, Phys. Rev. B **43**, 5713 (1991).

[8] H. J. M. Swagten, A. Twardowski, P. J. T. Eggenkamp, and W. J. M. de Jonge, Phys. Rev. B **46**, 188 (1992).

[9] J. Cisowski, Phys. Status Solidi B **111**, 289 (1982).

[10] G. C. de Vries, E. Frikkee, R. B. Helmholdt, K. Kopinga, and W. J. M. de Jonge, Physica B **156-157**, 321 (1989).

[11] G. C. de Vries, *Crystallographic and Magnetic Properties of* $(C_6D_{11}ND_3)CuBr_3$ *and* $(Zn_{1-x}Mn_x)_3As_2$*: A Neutron Scattering Study* (Netherlands Energy Research Foundation, Petten, 1989), p. 127.

[12] W. Lubczyński, J. Cisowski, H. Bednarski, J. Voiron, J. C. Portal, and J. C. Picoche, Acta Phys. Pol. A **77**, 175 (1990).

[13] W. Lubczyński, J. Cisowski, J. Kossut, and J. C. Portal, Semicond. Sci. Technol. **6**, 619 (1991).

[14] E. Lähderanta, R. Laiho, A. V. Lashkul, V. S. Zakhvalinskii, S. B. Roy, and A. D. Caplin, J. Magn. Magn. Mater. **104-107**, 1605 (1992); V. A. Kulbachinskii, I. V. Svistunov, S. M. Chudinov, V. D. Kuznetsov, E. K. Arushanov, V. S. Zakhvalinskii, and A. N. Nateprov, Fiz. Tekh. Poluprovodn. **25**, 2201 (1991) [Sov. Phys. Semicond. **25**, 1326 (1991)].

[15] S. M. Chudinov, V. A. Kulbachinskii, I. V. Svistunov, G. Mancini, and I. Davoli, Solid State Commun. **84**, 531 (1992).

[16] B. E. Larson, K. C. Hass, H. Ehrenreich, and A. E. Carlsson, Phys. Rev. B **37**, 4137 (1988).

[17] S. S. Yu and V. C. Lee, J. Phys. Condens. Matter **4**, 2961 (1992).

[18] Y. Shapira, S. Foner, D. Heiman, P. A. Wolff, and C. R. McIntyre, Solid State Commun. **70**, 355 (1989).

[19] C. J. M. Denissen, Ph.D. thesis, Eindhoven, The Netherlands, 1986.

[20] N. Bloembergen and T. J. Rowland, Phys. Rev. **97**, 1679 (1955).

[21] D. J. S. Beckett, S. F. Chebab, G. Lamarche, and J. C. Woolley, J. Magn. Magn. Mater. **69**, 311 (1987).

[22] J. Misiewicz and J. M. Pawlikowski, Solid State Commun. **32**, 687 (1979).

[23] J. Spałek, A. Lewicki, Z. Tarnawski, J. K. Furdyna, R. R.

Gałązka, and Z. Obuszko, Phys. Rev. B **33**, 3407 (1986).
[24]Y. Shapira, S. Foner, D. H. Ridgley, K. Dwight, and A. Wold, Phys. Rev. B **30**, 402 (1984).
[25]R. R. Gałązka, W. Dobrowolski, J. P. Lascaray, M. Nawrocki, A. Bruno, J. M. Broto, and J. C. Ousset, J. Magn. Magn. Mater. **72**, 174 (1988).
[26]A. Twardowski, P. Głód, W. J. M. de Jonge, and M. Demianiuk, Solid State Commun. **64**, 63 (1987).
[27]A. Twardowski, A. Lewicki, M. Arciszewska, W. J. M. de Jonge, H. J. M. Swagten, and M. Demianiuk, Phys. Rev. B **38**, 10 749 (1988).
[28]J. K. Furdyna and A. Samarth, J. Appl. Phys. **61**, 3526 (1987).
[29]W. J. M. de Jonge and H. J. M. Swagten, J. Magn. Magn. Mater. **100**, 322 (1991).
[30]A. Twardowski, H. J. M. Swagten, W. J. M. de Jonge, and M. Demianiuk, Phys. Rev. B **36**, 7013 (1987).
[31]M. Escorne and A. Mauger, Phys. Rev. B **25**, 4674 (1982).
[32]R. Sokel and W. A. Harrison, Phys. Rev. Lett. **36**, 61 (1976).
[33]S. Lara, R. M. Xavier, and C. A. Taft, J. Phys. Chem. Solids **39**, 247 (1978).
[34]G. Bastard and C. Lewiner, Phys. Rev. B **20**, 4256 (1979).
[35]V. C. Lee and L. Liu, Phys. Rev. B **29**, 2125 (1984).
[36]S. J. Frisken and D. J. Miller, Phys. Rev. B **33**, 7134 (1986).